Improved Targeting of Pancreatic Cancer: Experimental Studies of a New Bispecific Antibody, Pretargeting Enhancement System for Immunoscintigraphy

Thomas M. Cardillo,[1] Habibe Karacay,[1] David M. Goldenberg,[1] Dion Yeldell,[1] Chien-Hsing Chang,[2] David E. Modrak,[1] Robert M. Sharkey,[1] and David V. Gold[1]

[1]Garden State Cancer Center, Belleville, and [2]IBC Pharmaceutical Inc., Morris Plains, New Jersey

ABSTRACT

Purpose: **The early detection and diagnosis of pancreatic cancer remains a major clinical challenge in which imaging procedures have a central role. The purpose of this study was to evaluate a pretargeting method with a bispecific PAM4 (bsPAM4; anti-MUC1) antibody for radioimmunoscintigraphy of experimental human pancreatic cancer.**

Experimental Design: **A bispecific F(ab′)$_2$ antibody was generated from chimeric PAM4 Fab′ and murine 734 (anti-indium-diethylenetriaminepentaacetic acid) Fab′ fragments and then used in conjunction with 2 peptide haptens (^{111}In-IMP-156 and ^{99m}Tc-IMP-192). Biodistribution studies and radioimmunoscintigraphic imaging properties of the radiolabeled bsPAM4, and pretargeted, radiolabeled peptides were examined in the CaPan1 human pancreatic tumor grown as s.c. xenografts in athymic nude mice. Tumor uptake and tumor:nontumor ratios were compared with a nontargeting irrelevant anti-CD20, bispecific rituximab, radiolabeled peptides alone, and with directly labeled PAM4.**

Results: **Biodistribution results indicated significantly greater tumor uptake of radiolabeled peptides at 3 h after injection when pretargeting was performed with bsPAM4 as compared with the bispecific rituximab [20.2 ± 5.5 percentage of injected dose per gram of tissue (%ID/g) *versus* 0.9 ± 0.1%ID/g, respectively, for ^{111}In-IMP-156, and 16.8 ± 4.8%ID/g *versus* 1.1 ± 0.2%ID/g, respectively, for ^{99m}Tc-IMP-192]. Similar results were obtained at the 24-h time point. Tumor:nontumor ratios were >30 for all of the tissues except the kidneys, where a ratio of 7.8 ± 2.8 was observed. By immunoscintigraphy, tumors could be visualized as early as 30 min after injection of the radiolabeled peptide.**

Conclusions: **These studies demonstrate the feasibility of using the pretargeted, bispecific antibody technology for nuclear imaging of pancreatic cancer. The advantage of pretargeted bsPAM4 antibody as an imaging platform is the high specificity for pancreatic cancer as compared with the physicochemical parameters identified by current imaging technologies.**

INTRODUCTION

Pancreatic cancer represents a major health concern in the United States (1). In large part, this is because of our inability to detect and diagnose this disease at an early stage of development. Unfortunately, the usual clinical presentation for pancreatic cancer is at a late stage, when curative resection and/or other treatment modalities currently available hold little hope for a beneficial outcome. There are many factors that influence this outcome, including the nature of the disease itself (*i.e.*, its silent growth with nonspecific signs and symptoms that do not become evident until the tumor has grown quite large in volume), and technologies that must be improved to detect smaller-volume disease.

There have been considerable efforts toward development of a simple, cost-effective means for the early detection and diagnosis of pancreatic cancer. A major focus has been the generation of monoclonal antibodies (MAbs) that are able to distinguish cancer from normal and benign disease tissues and fluids. The CA19–9 immunoassay is the "gold standard," and although useful for management of the patient, it does not provide sufficient sensitivity or specificity to be used as a stand-alone diagnostic tool (2–4). Another more recent focus is the use of proteomics to identify a profile map in the serum, or other bodily fluid, that will distinguish pancreatic cancer from normal and other disease conditions (5, 6). The National Cancer Institute/FDA reports on the use of mass spectrometry to identify a peptide/protein profile that provides 100% sensitivity with 95% specificity for identification of ovarian cancer has provided enthusiasm for the potential of this technology (7, 8). Others are investigating many disease types, including pancreatic cancer, in efforts to identify disease-specific profiles (5, 6, 9–11). In addition to *in vitro* screening technologies, noninvasive imaging procedures currently in use provide additional support for an accurate diagnosis, as well as provide data regarding localization and staging to determine whether resection is an option. Computed tomography (12–14) and ultrasonography (15–17) are the most widely used technologies for imaging pancreatic cancer; however, detection of small tumors is problematic. Research is proceeding with magnetic resonance imaging as well as magnetic resonance cholangiopancreatography (18–20)

Received 10/3/03; revised 12/18/03; accepted 1/23/04.

Grant support: NIH Grants CA-54425 and CA92723 from the United States Public Health Service, and Grant DE-FG02–95ER62028 from the United States Department of Energy.

The costs of publication of this article were defrayed in part by the payment of page charges. This article must therefore be hereby marked *advertisement* in accordance with 18 U.S.C. Section 1734 solely to indicate this fact.

Note: T. Cardillo is currently at Immunomedics Inc., 300 American Way, Morris Plains, NJ 07950.

Requests for reprints: David V. Gold, Garden State Cancer Center, 520 Belleville Avenue, Belleville, NJ 07109. Phone: (973) 844-7025; Fax: (973) 844-7020; E-mail: dvgold@gscancer.org.

and positron emission tomography (PET; Refs. 21, 22) to provide increased sensitivity for the detection of malignant tissue.

Another useful tool for the diagnosis and staging of many different types of cancer is radioimmunoscintigraphy or radioimmunodetection. Radiolabeled antibodies specific for various tumor antigens have demonstrated their utility as imaging agents for hematological tumors (23–26), as well as for colorectal (27–29), medullary thyroid (30, 31), bladder (32), ovarian (33, 34), prostate (35), and breast cancers (36), among others. More recently, pretargeting methodologies have received a great deal of attention for imaging and therapy of cancer (37). The rationale for this approach is the superior tumor:nontumor (signal: noise) ratios that can be achieved, as compared with a directly labeled antibody or antibody fragment (37–40). The premise of the pretargeting approach is to decouple the targeting and imaging agents. An antitumor antibody, containing a second recognition site for a low molecular weight radiolabeled substance, is allowed to pretarget the tumor. At a later point in time when the targeting agent has cleared from the blood, the radiolabeled substance is injected. Due to its small size, the radiolabeled material is rapidly cleared from the blood and other normal tissues, whereas at the same time it is bound at the tumor by the second recognition site of the antibody construct. Two major approaches have been reported, the first using an antibody-avidin (or streptavidin) conjugate to pretarget the tumor, with radiolabeled-biotin (or biotin containing material) as the imaging agent (41–43), and the second, a bispecific antibody (bsMAb) construct, with one arm directed to tumor antigen and the other arm able to bind a subsequently administered radiolabeled-hapten (37, 38).

The primary attraction of a pretargeting system based on avidin-biotin is the very high affinity of avidin for biotin (41). However, there are some concerns with this technology, foremost being the immunogenicity of the avidin, which will inevitably restrict the number of times a patient can receive this reagent. Second is the fact that biotin is endogenous and can effectively reduce the subsequent targeting of the radiolabeled biotin. Although bispecific antibodies may not provide affinity interactions as high as the avidin-biotin system, the initial tumor targeting phase for each of the two approaches is equally dependent on the affinity of the antitumor antibody with tumor-expressed antigen. Also of importance, once humanized, the bispecific antibody should provide a lower immunogenic profile than avidin. Clinical trials using pretargeting procedures have demonstrated improved imaging of tumor sites compared with imaging with directly radiolabeled IgG antibodies (37, 39, 40, 44, 45).

Several forms of cancer, including pancreatic cancer, produce the MUC1 mucin glycoprotein (46–49). Overexpression of the antigen in malignant tissue has raised considerable interest in its use as a biomarker as well as a target for directed therapy. We have generated and characterized the anti-MUC1 MAb PAM4, providing both preclinical and clinical evidence as to its potential for radioimmunodetection and radioimmunotherapy of pancreatic cancer (50–53). Although there have been numerous reports on the development and application of anti-MUC1 antibodies, MAb PAM4, reactive with a defined epitope structure within MUC1, appears to have greater specificity for pancreatic cancer than other anti-MUC1 antibodies, most of which are reactive with the repeat domain (*e.g.,* HMFG1, SM3, BrE3, and so forth; Refs. 54–56). By immunohistochemistry, PAM4 was reactive with ~85% of pancreatic cancers, was nonreactive with normal adult pancreas, and gave only weak, yet positive, reactions with <25% of the pancreatitis specimens examined (50). Reverse transcription-PCR and Northern blot data have routinely confirmed that normal pancreatic tissue, as well as pancreatitis specimens, produce MUC1, albeit at much lower expression levels than is evident in pancreatic cancer (49, 57, 58). However, these methods do not consider post-translational modifications that may give rise to differing epitope structures. The relative specificity of PAM4 for MUC1 derived from pancreatic cancer is likely the consequence of differential glycosylation of the mucin protein core. MUC1 synthesized by different tissues, be they normal, benign, or malignant, may express different epitope structures due either to the direct presence of new or incomplete carbohydrate structures or the influence of carbohydrate structures on the tertiary conformation of the peptide core.

Initial clinical trials using ^{131}I- or ^{99m}Tc-labeled PAM4, whole IgG, revealed tumor targeting in 8 of 10 patients suspected of having pancreatic cancer (59, 60). Cancer was confirmed at surgery in all of the patients with targeted tumors. Of the 2 nontargeted patients, 1 had a poorly differentiated pancreatic cancer that did not express MUC1, whereas the other had pancreatitis rather than a malignant lesion. For the present studies, we hypothesized that a pretargeting approach using a PAM4-based bsMAb would provide increased tumor:nontumor ratios as compared with directly labeled PAM4 antibody for improved nuclear imaging of pancreatic cancer.

MATERIALS AND METHODS

Experimental Animal Model. CaPan1 is a human pancreatic carcinoma cell line obtained from the American Type Culture Collection (Manassas, VA). It was initially established as a solid tumor by injecting 10^7 cells s.c. into the right flank of 5-week-old female athymic *nu/nu* mice (Taconic, Germantown, NY). Once tumors had grown to ~1 cm^3, they were serially propagated by s.c. injection of 0.2 ml of a 20% (w/v) tumor suspension prepared by mincing the tumors in 0.9% saline with subsequent passage through a 40-mesh wire screen. CaPan1 cells produced moderately to well-differentiated tumors. Tumors used in this study were passaged <10 times. Animal studies were approved by the Center for Molecular Medicine and Immunology's Institutional Animal Care and Use Committee.

Construction of Bispecific Antibodies and Peptide Haptens. The purification and characterization of PAM4 has been described (50). Nontargeting, chimeric anti-CD20 rituximab and the murine anti-indium- diethylenetriaminepentacetic acid (DTPA) MAb, m734, were provided by Immunomedics, Inc. (Morris Plains, NJ). The production of antibody fragments and their subsequent use in the preparation of bsMAbs were performed as described previously (61). Briefly, F(ab′)$_2$ was derived by pepsin digestion of the MAb (cPAM4, chimeric rituximab, and m734) followed by protein A and ion-exchange chromatography purification. Fab′-SH fragments were formed by reduction of F(ab′)$_2$ fragments with 2-mercaptoethylamine.

The m734 Fab′-SH fragment was then converted to Fab′-maleimide by incubation with N,N′-*o*-phenylenedimaleimide. Fab′-SH fragments of cPAM4 or chimeric rituximab were mixed with m734-Fab′-maleimide at a 1:1 ratio and incubated overnight at 4°C. The resulting bsMAbs (bsPAM4 and bsRIT) were then purified on a size-exclusion high-performance liquid chromatography analytical column (Bio-Sil SEC-250; Bio-Rad, Richmond, CA). The final products gave a single peak on this same high-performance liquid chromatography column. The peptide haptens, IMP-156, to be radiolabeled with ^{111}In, and IMP-192 to be radiolabeled with ^{99m}Tc, were provided by Immunomedics, Inc. (61).

Radiolabeling of PAM4 IgG, Peptide Haptens, and bsMAbs. Sodium iodide-125, sodium iodide-131, and indium-111 chloride were obtained from NEN Life Science Products (Boston, MA). Sodium [^{99m}Tc]-pertechnetate was purchased from Mallinckrodt (Pine Brook, NJ). 1,4,7,10-Tetraazacyclododecane-*N*,*N*′,*N*″,*N*‴ -tetraacetic acid (Macrocyclics, Inc., Richardson, TX) was conjugated to cPAM4 IgG by a method described previously (62). A molar ratio of 3.3 1,4,7,10-tetraazacyclododecane-*N*,*N*′,*N*″,*N*‴ -tetraacetic acid molecules:IgG was determined by an ^{111}In-binding assay (63). Radiolabeling of the cPAM4 with ^{111}In-chloride, performed as described previously (52), yielded a product containing 1.7% unbound radiolabel and <1% aggregated material. The chloramine-T method was used for the radioiodination of the bsMAbs (64), with purification by size-exclusion columns eluted with 0.1 M sodium phosphate (pH 7.2) containing 0.15 M sodium chloride (PBS). Typically, radioiodinated products contained <1.5% aggregated material as determined by size-exclusion high-performance liquid chromatography and <1% unbound material as determined by instant TLC (ITLC-SG media; Pall Life Sciences, Ann Arbor, MI). IMP-192 was loaded with "cold" indium before the addition of ^{99m}Tc. The IMP-192 peptide was labeled with ^{99m}Tc and the IMP-156 peptide with ^{111}In, according to methods described previously (61, 62). Typically, radiolabeled peptides contained no aggregated material and <2% unbound radiolabel.

Bispecific MAb Biodistribution Studies. Athymic nude mice bearing s.c. CaPan1 human pancreatic cancer xenografts were coinjected with ^{125}I-bsPAM4 (10 μCi, 150 pmol, specific activity = 13.2 mCi/mg) and ^{131}I-labeled control, nontargeting bsRIT (35 μCi, 150 pmol, specific activity = 2.78 mCi/mg). At various time-points (4, 24, 36, 48, and 72 h after injection) groups of 5 mice were necropsied, and tumor and nontumor tissues were removed and counted in a gamma counter to determine percentage of injected dose per gram tissue (%ID/g).

Pretargeting Biodistribution Studies. Athymic nude mice bearing s.c. CaPan1 tumors were randomized into groups of 14 mice each. Two groups were injected with 10 μCi ^{125}I-labeled bsPAM4 (150 pmol, specific activity = 11.6 mCi/mg) whereas another two groups received 10 μCi ^{125}I-labeled control bsRIT (150 pmol, specific activity = 10.9 mCi/mg). After 40 h, one group of bsPAM4 and bsRIT pretargeted mice were injected with ^{111}In-IMP-156 (35 μCi; 15 pmol, specific activity = 4.95 mCi/nmol). The second group of bsPAM4 and bsRIT pretargeted mice were injected with ^{99m}Tc-IMP-192 (28 μCi; 15 pmol, specific activity = 2.10 mCi/nmol). Two remaining groups of mice received the radiolabeled peptides alone. Mice were necropsied at 3 and 24 h after injection of peptide, and their tumors and tissues removed and counted in a gamma counter to determine %ID/g.

Nuclear Imaging Studies. Experimental imaging studies were performed on mice bearing s.c. CaPan1 human pancreatic tumor xenografts. Groups of mice were administered unlabeled bsPAM4 or bsRIT (150 pmol). After 40 h, mice were injected with ^{111}In-IMP-156 (35 μCi, 15 pmol, specific activity = 2.29 mCi/nmol). Immediately after injection, the mice were placed in a Capintec CRC 15R dose calibrator (Ramsey, NJ) to confirm uniform doses present within the mice and to track whole body clearance of radiolabeled peptide. At various time points (0.5, 4, 24, 48, 120, and 168 h after administration), the mice were anesthetized, placed in the dose calibrator again to record overall activity, and imaged with a dual-head Solus gamma camera fitted with a medium-energy collimator for ^{111}In (ADAC Laboratories, Milipitas, CA). Mice were imaged for a total of 100,000 cpm or 10 min, whichever came first. As a means for comparison between the pretargeted and direct-labeled targeting procedures, a group of mice received ^{111}In-1,4,7,10-tetraazacyclododecane-*N*,*N*′,*N*″,*N*‴ -tetraacetic acid-cPAM4 whole IgG (35 μCi, specific activity = 0.88 mCi/mg). A final group received the radiolabeled peptide alone.

RESULTS

***In Vitro* Characterization of the bsMAbs.** Bispecific F(ab′)$_2$ antibodies were generated by chemically cross-linking the Fab′ fragment of murine anti-indium-DTPA, MAb m734, to the Fab′ fragment of either chimeric PAM4 (bsPAM4) or chimeric rituximab (bsRIT). High-performance liquid chromatography size-exclusion chromatography demonstrated a single peak for each bsMAb, with the molecular size equivalent to a 1:1 molar ratio of antitumor and anti-indium-DTPA fragments. The stability of the bsMAbs in fresh sterile-filtered mouse serum was analyzed over a period of 5 days, with no aggregation and/or degradation products evident by size-exclusion chromatography. *In vitro* and *in vivo* characteristics of the peptides, IMP-156 [Ac-Phe-Lys(DTPA)-Tyr-Lys(DTPA)-NH$_2$], for use with ^{111}In, and IMP-192 [Ac-Lys(DTPA)-Tyr-Lys(DTPA)-Lys(thiosemicarbazonyl-glyoxyl-cysteinyl-)-NH$_2$], for use with ^{99m}Tc, have been reported (61, 65). Each of the peptide haptens was divalent with respect to reactivity with MAb-m734 (anti-indium-DTPA). The antigen binding properties were examined by combining 1.5 pmol of bsPAM4 with 0.15 pmol of peptide (10:1 ratio, as was used for biodistribution and imaging studies) and an excess of MUC1 antigen, followed by incubation at 37°C for 1 h. This mixture was then applied to a column (0.5 × 60 cm) of Sepharose 4B-CL (Amersham Pharmacia Biotech, Piscataway, NJ) and eluted with PBS. Fractions of 0.5 ml were collected and counted in a Cobra II Auto-Gamma Counter (Packard Instruments, Meriden, CT). BsPAM4 bound 88% and 81% of the ^{111}In-IMP-156 and ^{99m}Tc-IMP-192, respectively (Fig. 1, *A* and *B*). Of the total ^{111}In-IMP-156 bound to bsPAM4, 92% eluted with the MUC1 fraction and 6% with the non-MUC1-reactive bsPAM4 fraction. An additional 2% of the radiolabeled peptide bound in a nonspecific manner to the MUC1 antigen. Of the total ^{99m}Tc-IMP-192 bound to bsPAM4, 85% eluted with the MUC1 fraction and 11% with the non-MUC1-reactive bsPAM4 fraction. An additional 4% of the

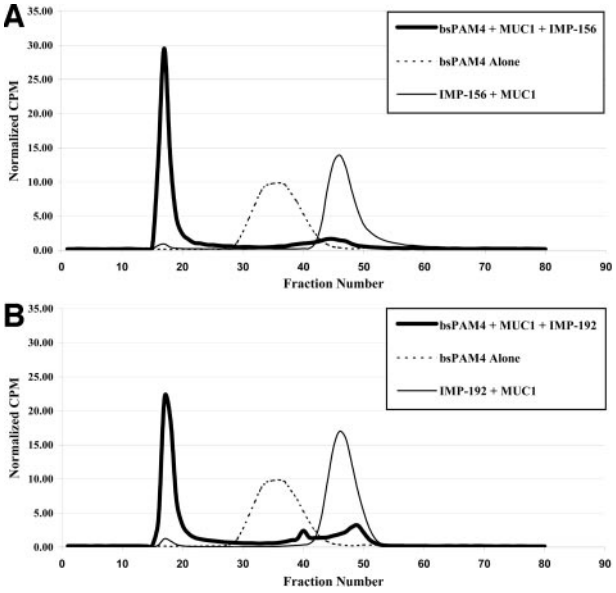

Fig. 1 Immunoreactivity of bispecific PAM4 (*bsPAM4*). Unlabeled bsPAM4 (1.5 pmol) was mixed with MUC1 (200 μg) and labeled peptide (0.15 pmol) for a final 10:1 ratio of bsPAM4 to peptide. Size exclusion chromatography was used to determine the percentage of immunoreactive fraction. *A,* elution patterns for bsPAM4 and ^{111}In-labeled IMP156 peptide; *B,* elution patterns for bsPAM4 and the ^{99m}Tc-labeled IMP192 peptide.

radiolabeled peptide bound in a nonspecific manner to the MUC1 antigen. bsRIT showed no evidence of reactivity with MUC1.

Biodistribution of the PAM4 bsMAb Alone. Athymic nude mice bearing s.c. CaPan1 human pancreatic tumors (~0.3 cm^3 at the start of the study) were coinjected with ^{125}I-labeled bsPAM4 antibody and a control, nontargeting ^{131}I-labeled bsRIT antibody. At various time points mice were necropsied, and the tumor and various tissues were removed and counted to determine the %ID/g. The concentration of radiolabeled bsPAM4 within the tumor was significantly greater than bsRIT at all time points (Fig. 2*A;* range for *P,* 0.0320–0.0098). Our past experience with a bispecific antibody pretargeting system suggested that a blood level of <1% ID/g was necessary to obtain high tumor:nontumor ratios of radiolabeled peptide (38, 49, 54). At 36 h after administration of the bsPAM4 there was 1.10 ± 0.40% ID/g in the blood (Fig. 2*B*), which fell to 0.56 ± 0.08% ID/g at 48 h postinjection. Concentration within the tumor at these time points was 6.43 ± 1.50% ID/g and 5.37 ± 2.38% ID/g, respectively. These values were significantly higher than the control bsRIT, which had 0.65 ± 0.33% ID/g and 0.47 ± 0.19% ID/g at 36 and 48 h ($P = 0.0180$ and $P = 0.0098$, respectively). Blood clearance rates (Fig. 2*B*) were not significantly different. Several statistically significant differences in the concentration of bsPAM4 and bsRIT were observed for nontumor tissues; however, in absolute terms these differences were minor. For example, at 24 h after injection there was significantly greater uptake of bsPAM4 than of bsRIT in the spleen (0.66 ± 0.06% *versus* 0.52 ± 0.02%; $P = 0.0412$), muscle (0.30 ± 0.04 *versus* 0.19 ± 0.02%; $P = 0.0169$), and blood (2.75 ± 0.17% *versus* 2.28 ± 0.10%; $P = 0.0241$).

Biodistribution of Bispecific PAM4 Targeted Peptides. On the basis of the biodistribution profile of the bsPAM4 antibody, pretargeting experiments were carried out in CaPan1 tumor-bearing mice (tumor volume ~0.3 cm^3 at the start of the study). Groups of mice were administered ^{125}I-bsPAM4 followed 40 h later by radiolabeled peptide hapten. One set of mice received ^{99m}Tc-labeled peptide, whereas a second set of mice received ^{111}In-labeled peptide. Controls for nonspecific targeting included two groups of mice that each received ^{125}I-bsRIT before administration of either ^{111}In- or ^{99m}Tc-labeled peptide and two other groups that received ^{111}In- or ^{99m}Tc-labeled peptide alone.

Fig. 3 presents the results obtained at 3 and 24 h after injection of peptide (43 and 64 h after administration of bsMAbs). Consistent with previous findings, there was significantly greater bsPAM4 in the tumors in comparison with the control nontargeting bsRIT, 8.2 ± 3.4% and 0.3 ± 0.08% ID/g, respectively ($P < 0.0001$). This translated into a significantly greater tumor uptake of ^{111}In-peptide in those mice administered bsPAM4 as compared with bsRIT (20.2 ± 5.5% ID/g *versus* 0.9 ± 0.1% ID/g, respectively; $P < 0.0001$) as well as tumor uptake of ^{99m}Tc-peptide (16.8 ± 4.8% ID/g *versus* 1.1 ± 0.2% ID/g, respectively; $P < 0.0005$). When administered without the advantage of pretargeted bsPAM4, radiolabeled peptides were rapidly cleared from the body with no specific targeting to

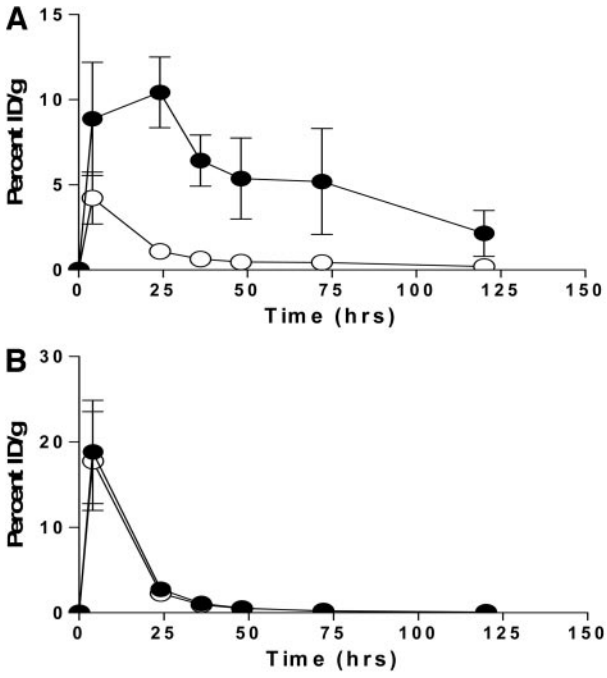

Fig. 2 Biodistribution of bispecific PAM4 (*bsPAM4*) antibody in tumor-bearing mice. Athymic nude mice bearing a human pancreatic cancer xenograft (CaPan1) were coinjected with ^{125}I-bsPAM4 and control, nontargeting ^{131}I-bispecific RIT (*bsRIT*). *A,* tumor uptake of radiolabeled bispecific monoclonal antibodies. *B,* blood clearance of the bispecific monoclonal antibodies from these same mice. ●, ^{125}I-bsPAM4; ○, ^{131}I-bsRIT; *bars,* ±SD.

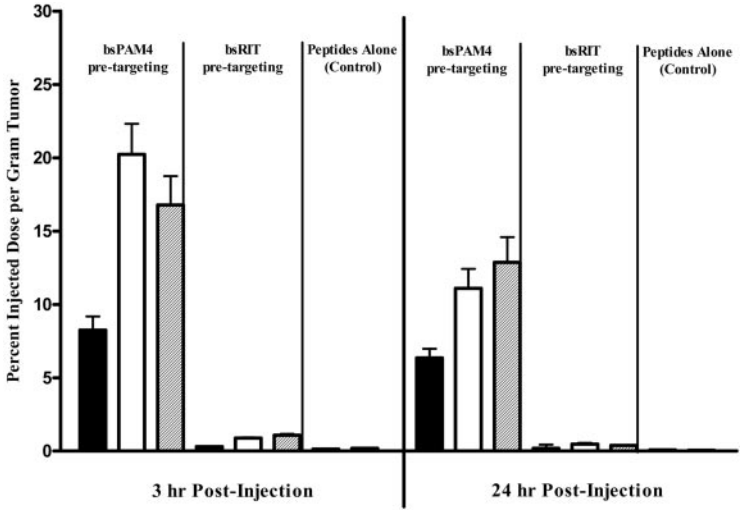

Fig. 3 Tumor uptake of radiolabeled peptides at 3 and 24 hours after injection. Athymic nude mice bearing CaPan1 tumors were administered 1.5×10^{-10} mol of ^{125}I-labeled bispecific (bs) monoclonal antibody (*bsPAM4* or *bsRIT*). After 40 h, the mice were injected with radiolabeled peptide (*^{111}In-IMP-156* or *^{99m}Tc-IMP-192*). Mice were necropsied at 3 and 24 h after administration of radiolabeled peptide (43 and 64 h after administration of bs monoclonal antibody), and the percentage of injected dose per gram of tissue within the tumors was determined. ■, bispecific antibody; □, ^{111}In-IMP-156; ▨, ^{99m}Tc-IMP-192; *bars,* ±SD.

tumor (0.2 ± 0.05% ID/g and 0.1 ± 0.03% ID/g for ^{99m}Tc-IMP-192 and ^{111}In-IMP-156; $P < 0.0004$ and $P < 0.0001$, respectively, in comparison to mice that had received pretargeted bsPAM4).

Table 1 presents the tumor:nontumor ratios for directly labeled bsPAM4 and each of the pretargeted radiolabeled peptides at an early time after administration of radiolabeled reagent. Overall, the pretargeted peptides gave significantly greater tumor:nontumor ratios for each of the tissues examined (range for *P* values: 0.0193 to <0.0001) than was observed for the direct-labeled bsPAM4 F(ab′)$_2$. Tumor:blood ratios were <2:1 for bsPAM4 F(ab′)$_2$. However, pretargeted ^{111}In-peptide and ^{99m}Tc-peptide provided significantly greater tumor:blood ratios equal to 36:1 and 9:1 [*P*s, <0.0001 and <0.008, respectively, when compared with direct-labeled bsPAM4 F(ab′)$_2$].

Similar results were observed at the 24-h postinjection time point (Fig. 3). A significantly greater concentration of bsPAM4 was noted in the tumor than was observed for the control bsRIT (6.4 ± 2.2% ID/g *versus* 0.2 ± 0.09% ID/g, respectively; $P < 0.0001$). This translated into higher concentrations of the radiolabeled peptides, 11.1 ± 3.5% ID/g and 12.9 ± 4.2% ID/g for ^{111}In- and ^{99m}Tc-labeled peptides in the tumors of mice pretargeted with bsPAM4 *versus* 0.5 ± 0.2% ID/g and 0.4 ± 0.03% ID/g in the tumors of mice that were given bsRIT ($P < 0.0008$ and $P < 0.0002$, respectively). Tumor uptake of radioisotope was significantly less when radiolabeled peptides were administered alone (^{99m}Tc-peptide, 0.06 ± 0.02% ID/g, $P < 0.0007$, and ^{111}In-peptide, 0.09 ± 0.02% ID/g, $P < 0.0002$) in comparison with the pretargeted methodology. The tumor:nontumor ratios at 24 h are presented in Table 2 with ^{111}In-labled cPAM4 whole IgG included for comparison. Each of the pretargeted radiolabeled peptides gave significantly higher tumor:nontumor values for all of the tissues examined when compared with those mice that received ^{111}In-cPAM4 whole IgG (range for *P* values, 0.048 to < 0.0001). Tumor:blood ratios for the pretargeted ^{111}In- and ^{99m}Tc-labeled peptides were significantly higher, 274:1 and 80:1, respectively, *versus* 4:1 for bsPAM4 F(ab′)$_2$ ($P < 0.0002$) and 2:1 for ^{111}In-cPAM4 IgG ($P < 0.0002$).

Nuclear Imaging Studies. Athymic nude mice bearing CaPan1 tumor xenografts (~0.15 cm^3 at the start of the study)

Table 1 Tumor:nontumor ratios based on the biodistribution of pretargeted peptides or antibody fragments at 3 h postadministration

	Pretargeted ^{111}In-peptide (3 h)		Pretargeted ^{99m}Tc-peptide (3 h)		^{125}I-bsPAM4 F(ab′)$_2$ (4 h)	
Tissue	Mean	(±SD)	Mean	(±SD)	Mean	(±SD)
Liver	36.1	11.7	16.7	7.2	2.3	0.6
Spleen	33.4	20.6	14.6	9.1	2.2	0.7
Kidney	7.8	2.8	8.1	3.3	1.1	0.2
Lung	44.6	13.0	15.8	5.9	1.6	0.4
Blood	36.5	8.3	9.9	5.2	0.5	0.1
Bone	123.2	40.0	ND	ND	ND	ND
Washed bone	378.0	124.6	ND	ND	ND	ND
Pancreas	155.6	30.1	73.3	32.9	4.7	1.2
Tumor (g)	0.189	(0.070)	0.174	(0.050)	0.179	(0.139)
Tumor %ID/g[a]	20.2	(5.5)	16.8	(4.8)	8.9	(3.3)

[a] %ID/g, percentage of injected dose per gram of tissue.

Table 2 Tumor:nontumor ratios based on the biodistribution of pretargeted peptides or antibody fragments at 24 h postadministration

	Pretargeted ^{111}In-peptide		Pretargeted ^{99m}Tc-peptide		^{125}I-bsPAM4 F(ab′)$_2$		^{111}In-cPAM4 IgG	
Tissue	Mean	(±SD)	Mean	(±SD)	Mean	(±SD)	Mean	(±SD)
Liver	26.3	10.4	24.3	5.5	16.9	1.7	3.5	1.6
Spleen	33.1	14.0	24.2	10.0	15.8	2.8	3.8	2.0
Kidney	8.4	1.7	16.2	5.2	8.6	1.2	5.9	1.3
Lung	101.1	37.9	52.5	17.7	8.1	0.4	5.6	1.9
Blood	274.1	89.6	80.8	20.4	3.8	0.5	2.4	1.0
Bone	144.2	23.8	ND	ND	ND	ND	13.2	6.1
Washed bone	256.2	59.9	ND	ND	ND	ND	25.1	14.2
Pancreas	244.6	74.5	873.8	305.7	18.0	0.3	18.6	8.2
Tumor (g)	0.192	(0.079)	0.235	(0.139)	0.131	(0.064)	0.256	(0.097)
Tumor %ID/g[a]	11.1	(3.5)	12.9	(4.2)	10.4	(2.1)	22.8	(6.9)

[a] %ID/g, percentage of injected dose per gram of tissue.

were administered the bsPAM4 followed by ^{111}In-peptide to target and image the tumors. The control groups included one that received a similarly administered bsRIT followed by ^{111}In-peptide, a group that received only the ^{111}In-peptide, and a final group that was administered ^{111}In-cPAM4 IgG. Whole-body clearance of ^{111}In from mice administered the pretargeted radiolabeled peptide was rapid in comparison to those mice administered ^{111}In-cPAM4 IgG (Fig. 4). Greater than 85% of the radiolabeled peptide was cleared within 4 h postinjection *versus* only 18% for the radiolabeled PAM4 IgG at this same time point. Whole-body activity fell to <1 μCi at 48 h for the pretargeted ^{111}In peptide (0.73 ± 0.43 μCi), whereas even at 7 days, there was >1 μCi still present in the mice injected with ^{111}In-cPAM4 IgG (2.1 ± 1.8 μCi). This residual activity was detected in the abdominal region of the mice.

For those mice pretargeted with bsPAM4, tumors could be visualized at the earliest time points of 0.5 and 4 h, but clearance of unbound peptide was prominent within the kidneys and bladder. Continued imaging of the bsPAM4 pretargeted group at 24–168 h demonstrated long-term retention of the radiolabeled peptide within the tumor, with minimal background activity. A comparison of the images taken at 48 h after administration of radiolabeled agent demonstrated clear, specific tumor imaging for the group of mice given bsPAM4 as a pretargeting agent (Fig. 5). Although tumor is evident in 1 of the mice injected with ^{111}In-cPAM4 IgG, high background activity in the thoracic and abdominal regions can be seen in both animals. None of the mice pretargeted with control bsRIT or injected with radiolabeled peptide alone showed evidence of targeting to tumor.

DISCUSSION

Radiolabeled antibodies have been used for imaging numerous malignancies, including hematological (23–26), colorectal (27–29), ovarian (33, 34), and breast (36) tumors. This technology may also prove useful for pancreatic cancer. However, other than the application of anticarcinoembryonic antigen (66) and B72.3/CC49 antibodies (67, 68), little clinical information exists. Our results with radiolabeled PAM4 targeting to experimental pancreatic tumor compare quite favorably with the results of targeting studies reported with antibodies reactive with carcinoembryonic antigen (69, 70), CA19–9 (70, 71), CA125 (70), and other antigens within pancreatic cancer (72, 73). Our initial clinical studies with radiolabeled murine PAM4 were promising, because a majority of the lesions were targeted in all of the patients without appreciable uptake in normal

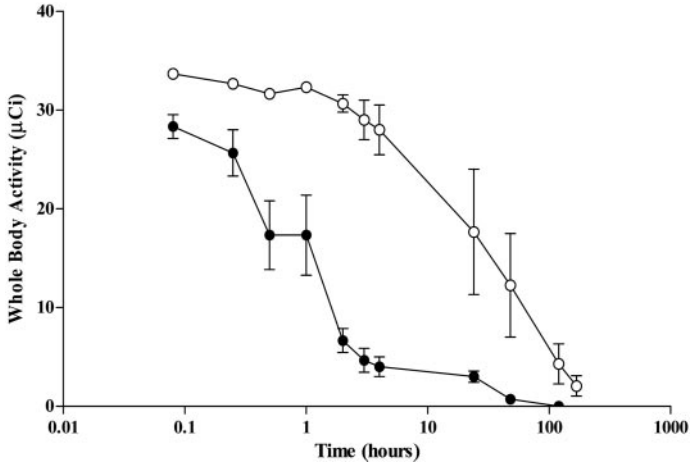

Fig. 4 Whole body clearance of bispecific PAM4 (*bsPAM4*)-targeted ^{111}In-IMP-156 peptide *versus* ^{111}In-1,4,7,10-tetraazacyclododecane-*N*,*N*′,*N*″,*N*‴ -tetraacetic acid-cPAM4 whole IgG. Athymic nude mice bearing s.c. CaPan1 tumor xenografts were either pretargeted with bsPAM4 for 40 h before the administration of ^{111}In-labeled peptide or were injected with ^{111}In-labled cPAM4 IgG. At various time points the mice were placed in a dose calibrator and total activity determined. ○, ^{111}In-cPAM4 IgG; ●, bsPAM4-pretargeted ^{111}In-peptide; *bars*, ±SD.

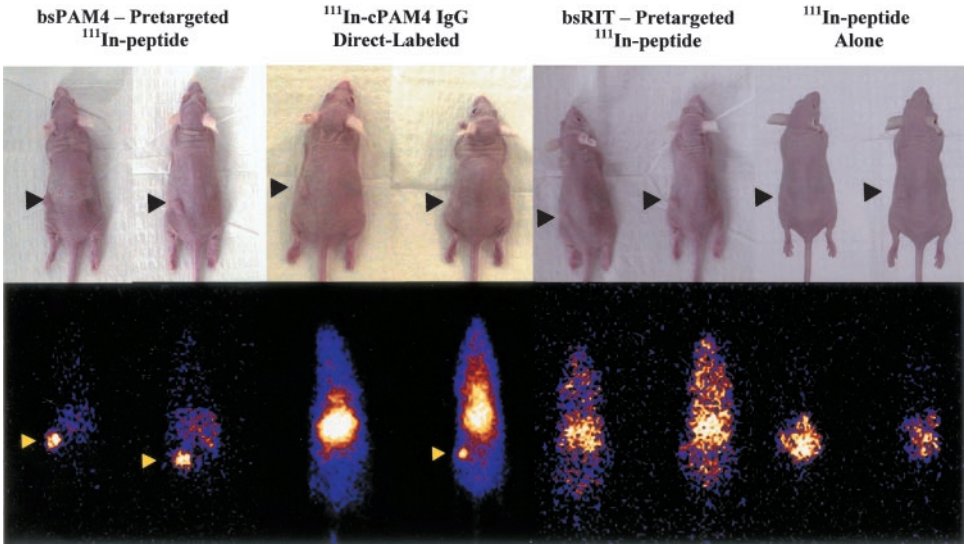

Fig. 5 Immunoscintigraphy of pancreatic tumor xenografts. Athymic nude mice bearing CaPan1 tumor xenografts were injected with bispecific PAM4 (*bsPAM4*; 1.5×10^{-10} mol) followed by administration of ^{111}In-peptide (35 μCi; 1.5×10^{-11} mol) 40 h later. A comparison of the images taken at 48 h after injection of radiolabeled peptide was made between these mice and mice that were injected with ^{111}In-cPAM4 whole IgG, or pretargeted with control bsRIT, or given radiolabeled peptide alone.

tissues (59, 60). Of particular note, specificity was demonstrated in that PAM4 did not target a case that was, in fact, active pancreatitis rather than pancreatic cancer.

Radioimmunoscintigraphy of solid tumors has been hampered by the low, heterogeneous uptake of the antibodies in target tumors and by the long serum half-life of the labeled antibodies (74). Thus, signal:noise ratios are low for image processing. Reduction of undesirably high background radioactivity has been approached in several ways. One method has been to reduce the molecular size of the MAb, first by removing the Fc fragment to generate F(ab′)$_2$, and also, further reduction to Fab′ or Fab species. MAb fragments are cleared more rapidly from the blood, but they also present lower uptake within tumor and higher activity within the kidney (75). Even smaller targeting moieties, such as single chain antibodies (scFv), have been made, but absolute tumor uptake is reduced still further from that observed with whole IgG targeting agents (76). The smaller molecules are better able to penetrate tumors, providing a more uniform distribution (41, 77); nevertheless, it is the concentration of radioisotope within the tumor, as well as signal:noise ratio, that are important for detection of small volume disease.

An alternate approach involves pretargeting methodologies. Two antibody-based pretargeting approaches have been reported, one involving the use of an avidin or streptavidin-biotin targeting system and the other a bsMAb approach. In each system, the primary targeting MAb carries a secondary recognition moiety, which itself is targeted later with a radiolabeled hapten (*e.g.*, biotinylated chelate, chelate alone, or a small peptide-conjugated chelate). The small molecular size of the hapten makes it ideally suited for rapid tumor penetration (77), and if designed properly, it should clear from the body rapidly without significant residual uptake in nontargeted tissues.

In this report, our aim was to determine the feasibility of a pretargeted PAM4-based bispecific antibody for nuclear imaging of pancreatic cancer. At 3 h after administration of radiolabeled peptide, >16% ID/g was observed in the tumor for ^{111}In-and ^{99m}Tc-labeled peptides. The high concentration of radioisotope within the tumor is an important factor for detection of small-volume disease. Both of the pretargeted peptides gave significantly higher tumor:nontumor ratios than was achieved with directly radiolabeled PAM4 F(ab′)$_2$ or PAM4 whole IgG. Even 24 h after peptide administration, we observed >10% ID/g of radiolabeled peptide in the tumors. The lowest tumor:nontumor ratios observed were for the kidney, although the ratios were still quite high at ~8:1. This was not unexpected, because the small peptide haptens are cleared primarily through the kidneys. Whereas not addressed in this study, the administration of certain amino acids (*e.g.*, D-lysine) before injection of radiolabeled peptide can inhibit retention of radioactivity in the kidneys without altering tumor uptake (78, 79). This could be of particular importance if the bsPAM4 pretargeting system is to be considered as a therapeutic for pancreatic cancer.

To demonstrate the utility of the pretargeted bsPAM4 system for imaging, radioimmunoscintigraphy was performed in mice bearing human pancreatic tumor xenografts. Imaging data confirmed the rapid tumor uptake of radiolabeled peptide with tumors visible as early as 30 min after injection. On the other hand, mice that were given ^{111}In-labeled PAM4 whole IgG had sufficient activity in the blood such that tumors were obscured until later time points. Likewise, Boerman *et al.* (80), using a similar pretargeting system, showed rapid tumor targeting of a renal carcinoma xenograft with clear identification of tumors by 4 h after administration of radiolabeled peptide. By 48 h, very little background radiation was present. Le Doussal *et al.* (81) obtained similar results with their bsMAb for targeting melanoma. Both studies demonstrated that the pretargeted bsMAb approach was superior to administration of a directly radiolabeled whole IgG.

It is important to note that as a platform technology, the peptide hapten can be adapted to other imaging methodologies, as for example the use of positron emitters for PET imaging. This technology can provide greater sensitivity when compared with γ-emitting detection systems, but, as it is most frequently performed, using ^{15}F-fluorodeoxyglucose, the hypermetabolic

activity of cancer tissue is the underlying basis for discrimination between malignant and benign/normal tissue (82). Based solely on metabolic activity, there is the potential for inflammatory processes to yield false positive results. On the other hand, antibody-based PET imaging agents may provide specificity for improved discrimination of tumor and nontumor tissues. The feasibility of this approach has been demonstrated by use of a bispecific anti-MUC1/anti-Ga chelate antibody in a pretargeting system with ^{68}Ga-radiolabeled hapten for immuno-PET imaging of breast cancer (83, 84). In preclinical biodistribution studies, tumor:nontumor ratios were reported to be higher for the pretargeted methodology as compared with the directly labeled whole IgG or its fragments. Tumors were clearly visualized by PET imaging at 1 h after injection of radiolabeled hapten. An initial clinical study confirmed these results, with detection of tumors as small as 10 mm in size, and with tumor:normal breast ratios of as little as 2 (84). These reports, along with the results presented here, provide the rationale for pursuit of bsPAM4 pretargeting for PET imaging of pancreatic cancer.

Another important finding in this study was the extended retention of radiolabeled peptide within the tumor over the 7-day study period. The high tumor:nontumor ratios, coupled with the high concentration of radiolabeled hapten within the tumor, suggest that this technology may also have therapeutic applications. Although we have used ^{111}In as the imaging agent, substitution with ^{90}Y may provide significant therapeutic effects. We reported previously cures of large (1 cm^3) xenografted pancreatic tumors by radioimmunotherapy with ^{90}Y-PAM4 whole IgG (52). We have also reported studies on the use of gemcitabine combined with ^{90}Y-PAM4 whole IgG radioimmunotherapy (53). Whereas gemcitabine given alone had no antitumor effect in the large tumors examined, addition of a low-dose of ^{90}Y-PAM4 ($\sim$10% of the maximum tolerated dose) to a standard regimen of gemcitabine enhanced the antitumor effect significantly. Hematological toxicity is, of course, an issue for gemcitabine, as well as for directly radiolabeled whole IgG. However, the data presented in the current studies suggest that a pretargeted bsPAM4 approach may provide substantially less hematological toxicity as compared with use of directly labeled whole IgG. Due to the rapid clearance of the radiolabeled hapten in a pretargeting regimen, the dose-limiting organ is more likely to be the kidney, although, even for this organ, the data suggest that there may be minimal toxicity (2.7 + 0.4%ID/g at 3 h and 1.3 + 0.2%ID/g at 24 h for ^{111}In-labeled peptide haptens). The combined use of gemcitabine and pretargeted radioimmunotherapy treatment modalities, having non-overlapping toxicities, may provide superior antitumor effects, with a better toxicity profile than was observed for the gemcitabine and PAM4-IgG radioimmunotherapy treatment. These studies are in progress.

In conclusion, we have demonstrated the feasibility of using the pretargeted, bispecific antibody technology for nuclear imaging of pancreatic cancer. The advantage of the pretargeted bsPAM4 antibody as an imaging platform is the achievement of very high tumor:nontumor ratios early after injection of the radiolabeled hapten. Use of the MUC1-reactive PAM4 antibody should result in a high specificity for pancreatic cancer as compared with the physicochemical parameters identified by current imaging technologies. At the present time, we envision that this imaging technology might be useful as part of a paradigm for initial diagnosis and imaging of patients suspected of pancreatic cancer, as well as a sensitive method for determining extent of disease. Prospective clinical trials are required to test this thesis.

REFERENCES

1. American Cancer Society, Cancer Facts and Figures, 2003. Atlanta: American Cancer Society, 2003. p. 16.
2. Ritts RE, DelVillano B, Go VLW, Herberman RB, Lug TL, Zurawski VR. Initial clinical evaluation of an immunoradiometric assay for CA19–9 using the NCI serum bank. Int J Cancer 1984;33:339–45.
3. Steinberg W. The clinical utility of the CA19–9 tumor associated antigen. Am J Gastroenterol 1990;85:350–5.
4. Ritts RE, Pitt HA. CA19–9 in pancreatic cancer. Surg Oncol Clin North Am 1998;7:93–101.
5. Koopman J, Zhang Z, White N, et al. SELDI approach for biomarker identification in the diagnosis of pancreatic adenocarcinoma. Proc Am Assoc Cancer Res 2003;44:1143.
6. Chen G, Yu Y, Chen S, Zhang W, Xu, Y. Serum fingerprinting as novel biomarkers for detecting pancreatic cancer. Proc Am Assoc Cancer Res 2003;44:1361.
7. Petricoin EF, Ardekani AM, Hitt BA, et al. Use of proteomic patterns in serum to identify ovarian cancer. Lancet 2002;359:572–7.
8. Liotta LA, Petricoin EF, Ardenkani AM, et al. General keynote: proteomic patterns in sera serve as biomarkers of ovarian cancer. Gynecol Oncol 2003;88:S25–8.
9. Lawrie LC, Curran S, McLeod HL, Fothergill JE, Murray GI. Application of laser capture microdissection and proteomics in colon cancer. Mol Pathol 2001;54:253–8.
10. Adam B-L, Qu Y, Davis JW, et al. Serum protein fingerprinting coupled with a pattern-matching algorithm distinguishes prostate cancer from benign prostate hyperplasia and healthy men. 2002;62:3609–14.
11. Dwek MV, Alaiya AA. Proteome analysis enables separate clustering of normal breast, benign breast and breast cancer tissues. Br J Cancer 2003;89:305–7.
12. Bluemke DA, Cameron JL, Hruban RH, et al. potentially resectable pancreatic adenocarcinoma:spiral CT assessment with surgical and pathological correlation. Radiology 1995;197:381–5.
13. Irie H, Honda H, Kaneko K, Kuroiwa T, Yoshimitsu K, Masuda K. Comparison of helical CT and MR imaging in detecting and staging small pancreatic adenocarcinoma. Abdom Imaging 1997;22:429–33.
14. Hough TJ, Raptopoulos V, Siewert B, Matthews JB. Teardrop superior mesenteric vein: CT sign for unresectable carcinoma of the pancreas. AJR Am J Roentgenol 1999;173:1509–12.
15. Bennett GL, Hann LE. Pancreatic ultrasonography. Surg Clin North Am 2001;81:259–81.
16. Bottger TC, Boddin J, Duber C, Heintz A, Kuchle R, Junginger T. Diagnosing and staging of pancreatic carcinoma – what is necessary? Oncology 1998;55:122–9.
17. Ariyama J, Suyama M, Satoh K, Wakabayashi K. Endoscopic ultrasound and intraductal ultrasound in the diagnosis of small pancreatic tumors. Abdom Imaging 1998;23:380–6.
18. Fayad LM, Mithcell DG. Magnetic resonance imaging of pancreatic adenocarcinoma. Int J Gastroent Cancer 2001;30:19–25.
19. Ly JN, Miller FH. MR imaging of the pancreas: a practical approach. Radiol Clin North Am 2002;40:1289–306.
20. Talamonti MS, Denham W. Staging and surgical management of pancreatic and biliary cancer and inflammation. Radiol Clin North Am 2002;40:1397–410.
21. Freeny PC. Pancreatic carcinoma: imaging update 2001. Dig Dis 2001;19:37–46.

22. Chin BB, Wahl RL. ^{18}F-Fluoro-2-deoxyglucose positron emission tomography in the evaluation of gastrointestinal malignancies. Gut 2003;4 (suppl):23–9.

23. Sohn SK, Ahn BC, Lee SW, et al. Bone marrow immunoscintigraphy using technetium-99m anti-granulocyte antibody in multiple myeloma. Eur J Nucl Med Mol Imaging 2002;29:591–6.

24. Krause T, Eisenmann N, Reinhardt M, et al. Bone marrow scintigraphy using technetium-99m antigranulocyte antibody in malignant lymphomas. Ann Oncol 1999;10:79–85.

25. Behr TM, Holler E, Gratz S, et al. CD22 is a suitable target molecule for detection and high-dose, myeloablative radioimmunotherapy with the monoclonal antibody LL2 in acute lymphatic leukemia and Waldenström's macroglobulinaemia. Tumor Targeting 1998;3:32–40.

26. Gasparini M, Bombardieri E, Tondini C, et al. Clinical utility of radioimmunoscintigraphy of non-Hodgkin's lymphoma with radiolabeled LL2 monoclonal antibody, LymphoSCAN: preliminary results. Tumori 1995;81:173–8.

27. Hladik P, Vizda J, Bedrna J, et al. Immunoscintigraphy and intraoperative radioimmunodetection in the treatment of colorectal carcinoma. Colorectal Dis 2001;3:380–6.

28. Lechner P, Lind P, Goldenberg DM. CEA immunoscintigraphy detects resectable rectal cancer recurrence and improves survival. Coloproctology 2000;22:23–8.

29. Lechner P, Lind P, Goldenberg DM. Can postoperative surveillance with serial CEA immunoscintigraphy detect resectable rectal cancer recurrence and potentially improve tumor-free survival? J Am Coll Surg 2000;191:511–8.

30. Juweid M, Sharkey RM, Behr TM, et al. Improved detection of medullary thyroid cancer with radiolabeled antibodies to carcinoembryonic antigen. J Clin Oncol 1996;14:1209–17.

31. Juweid M, Sharkey RM, Swayne LC, Goldenberg DM. Improved selection of patients for reoperation for medullary thyroid cancer by imaging with radiolabeled anticarcinoembryonic antigen antibodies. Surgery 1997;122:1156–65.

32. Wang R, Zhang C, Yu L, Guo Y. Clinical application of radioimmunoimaging with ^{99m}Tc-BDI-1 in the diagnosis of bladder cancer. Chin Med J (Engl) 2000;113:396–9.

33. Kalofonos HP, Karamouzis MV, Epenetos AA. Radioimmunoscintigraphy in patients with ovarian cancer. Acta Oncol 2001;40:549–57.

34. Kalofonos HP, Giannakenas C, Kosmas C, et al. Radioimmunoscintigraphy in patients with ovarian cancer. Acta Oncol 1999;38:629–34.

35. Manyak MJ, Hinkle GH, Olsen JO, et al. Immunoscintigraphy with indium-111-capromab pendetide: evaluation before definitive therapy in patients with prostate cancer. Urology 1999;54:1058–63.

36. Goldenberg DM, Nabi HA, Sullivan CL, et al. Carcinoembryonic antigen immunoscintigraphy complements mammography in the diagnosis of breast cancer. Cancer 2000;89:104–15.

37. Chang, C-H, Sharkey RM, Rossi EA, et al. Molecular advances in pretargeting radioimmunotherapy with bispecific antibodies. Mol Cancer Ther 2002;1:553–63.

38. Sharkey RM, McBride WJ, Karacay H, et al. A universal pretargeting system for cancer detection and therapy using bispecific antibody. Cancer Res 2003;63:354–63.

39. Vuillez J Ph, Moro D, Brichon PY, et al. Two-step immunoscintigraphy for non-small cell lung cancer staging using a bispecific anti-CEA/anti-indium-DTPA antibody and an indium-111-labeled DTPA dimer. J Nucl Med 1997;38:507–11.

40. Le Doussal J-M, Chetanneau A, Gruaz-Guyon A, et al. Bispecific monoclonal antibody-mediated targeting of an indium-111-labeled DTPA dimer to primary colorectal tumors: Pharmacokinetics, biodistribution, scintigraphy and immune response. J Nucl Med 1993;34:1662–71.

41. Hnatowich DJ, Virzi F, Rusckowski M. Investigations of avidin and biotin for imaging applications. J Nucl Med 1987;28:1294–302.

42. Karacay H, Sharkey RM, Govindan SV, et al. Development of a streptavidin-anti-carcinoembryonic antigen antibody, radiolabeled biotin pretargeting method for radioimmunotherapy of colorectal cancer Reagent development Bioconj Chem 1997;8:585–94.

43. Sharkey RM, Karacay H, Griffiths GL, et al. Development of a streptavidin-anti-carcinoembryonic antigen antibody, radiolabeled biotin pretargeting method for radioimmunotherapy of colorectal cancer. Studies in a human colon cancer xenograft model. Bioconj Chem 1997;8:595–604.

44. Peltier P, Curtet C, Chatal J-F, et al. Radioimmunodetection of medullary thyroid cancer using a bispecific anti-CEA/anti-indium-DTPA bispecific antibody and an indium-111-labeled dimer. J Nucl Med 1993;34:1267–73.

45. Barbet J, Peltier P, Bardet S, et al. Radioimmunodetection of medullary thyroid carcinoma using indium-111 bivalent hapten and anti-CEA x anti-DTPA-indium bispecific antibody. J Nucl Med 1998; 39:1172–8.

46. Kim YS, Gum J Jr., Brockhausen I. Mucin glycoproteins in neoplasia Glycoconj J 1996;13:693–707.

47. Gendler SJ. MUC1, the renaissance molecule. J Mammary Gland Biol Neoplasia 2001;6:339–53.

48. Taylor-Papadimitriou J, Burchell JM, Plunkett T, et al. MUC1 and the immunobiology of cancer. J Mammary Gland Biol Neoplasia 2002; 7:209–21.

49. Ringel J, Lohr M. The MUC gene family: Their role in diagnosis and early detection of pancreatic cancer. Mol Cancer 2003;2:9.

50. Gold DV, Lew K, Maliniak R, Hernandez M, Cardillo T. Characterization of monoclonal antibody PAM4 reactive with a pancreatic cancer mucin. Int J Cancer 1994;57:204–10.

51. Gold DV, Alisauskas R, Sharkey RM. Targeting of xenografted pancreatic cancer with a new monoclonal antibody, PAM4. Cancer Res 1995;55:1105–10.

52. Cardillo TM, Ying Z, Gold DV. Therapeutic advantage of (90)yttrium- versus (131)iodine-labeled PAM4 antibody in experimental pancreatic cancer. Clin Cancer Res 2001;7:3186–92.

53. Gold DV, Schutsky K, Modrak D, Cardillo TM. Low-dose radioimmunotherapy ((90)Y-PAM4) combined with gemcitabine for the treatment of experimental pancreatic cancer. Clin Cancer Res 2003;9: 3929S–37S.

54. Berry N, Jones DB, Smallwood J, Taylor I, Kirkham N, Taylor-Papadimitriou J. The prognostic value of the monoclonal antibodies HMFG1 and HMFG2 in breast cancer. Br J Cancer 1985;51:179–86.

55. Granowska M, Mather SJ, Jobling T, et al. Radiolabelled stripped mucin, SM3, monoclonal antibody for immunoscintigraphy of ovarian tumours. Int J Biol Markers 1990;5:89–96.

56. Peterson JA, Zava DT, Duwe AK, Blank EW, Battifora H, Ceriani RL. Biochemical and histological characterization of antigens preferentially expressed on the surface and cytoplasm of breast carcinoma cells identified by monoclonal antibodies against the human milk fat globule. Hybridoma 1990;9:221–35.

57. Hollingsworth MA, Strawhecker JM, Caffrey TC, Mack DR. Expression of MUC1, MUC2, MUC3 and MUC4 mucin mRNAs in human pancreatic and intestinal tumor cell lines. Int J Cancer 1994;57:198–203.

58. Andrianifahanana M, Moniaux N, Schmied BM, et al. Mucin (MUC) gene expression in human pancreatic adenocarcinoma and chronic pancreatitis: a potential role of MUC4 as a tumor marker of diagnostic significance. Clin Cancer Res 2001;7:4033–40.

59. Mariani G, Molea N, Bacciardi D, et al. Initial targeting, biodistribution and pharmacokinetics screening of the monoclonal antibody PAM 4 for immunoscintigraphy in patients with pancreatic cancer. Cancer Res 1995;55:5911s–5s.

60. Gold DV, Cardillo T, Goldenberg DM, Sharkey RM. Localization of pancreatic cancer with radiolabeled monoclonal antibody PAM4. Crit Rev Hematol/Oncolo 2001;39:147–54.

61. Karacay H, McBride WJ, Griffiths GL, et al. Experimental pretargeting studies of cancer with a humanized anti-CEA x murine anti-[In-DTPA] bispecific antibody construct and a Tc-99m/Re-188 labeled peptide. Bioconj Chem 2000;11:842–54.

62. Govindan SV, Shih LB, Goldenberg DM, et al. 90-Yttrium-labeled complementarity-determining-region-grafted monoclonal antibodies for radioimmunotherapy: radiolabeling and animal biodistribution studies. Bioconjug Chem 1998;9:773–82.

63. Cummins DH, Rutter EW Jr, Fordyce WA. A convenient synthesis of bifunctional chelating agents based on diethylenetriaminepentaacetic acid and their coordination chemistry Bioconj Chem 1991;2:180–6.

64. McConahey PJ, Dixon FJ. A method of trace iodination of proteins for immunologic studies. Int Arch Allergy Appl Immunol 1966;29: 185–9.

65. Karacay H, Sharkey RM, McBride WJ, et al. Pretargeting for cancer radioimmunotherapy with bispecific antibodies: Role of the bispecific antibody's valency for the tumor target antigen. Bioconj Chem 2002; 13:1054–70.

66. Hajjar G, Sharkey RM, Burton J, et al. Phase I radioimmunotherapy trial with iodine-131-labeled humanized MN-14 anti-carcinoembryonic antigen monoclonal antibody in patients with metastatic gastrointestinal and colorectal cancer. Clin Colorectal Cancer 2002;2:31–42.

67. LaValle GJ, Martinez DA, Sobel D, DeYoung B, Martin EW. Jr. Assessment of disseminated pancreatic cancer: a comparison of traditional exploratory laparotomy and radioimmunoguided surgery. Surgery 1997;122:867–71.

68. Kaufmann LW, Vaillant JC, van Gulik TM, van Royen EA, Parc R, Obertop H. Efficacy of monoclonal antibody 131I-B72.3 immunoscintigraphy of pancreatic adenocarcinoma xenografts in nude mice. Eur J Surg 1999;165:659–64.

69. Goldrosen MH, Loftus R, Lloyd F, et al. Localization of monoclonal antibody in a novel nude mouse model of pancreatic cancer. Proc Am Assoc Cancer Res 1988;29:419.

70. Klapdor R, Montz R, Greten H, et al. Immunszintigraphie und Radioimmuntherapie des transpantierten Pankreaskarzinoms. Nucl Med 1985;124:227–31.

71. Senekowitsch R, Maul FD, Baum RP, et al. Immunoscintigraphy of human pancreatic carcinoma in nude mice with $F(ab')_2$ fragments of monoclonal antibodies to CA19–9 and CEA. In: C. Winkler, editor. Nuclear Medicine in Clinical Oncology: Current Status and Future Aspects, New York: Springer Verlag, 1986. p. 391–6.

72. Nakamura K, Kubo A, Hashimoto S, Furuchi T, Takami H, Abe O. Radioimmunodetection of human pancreatic tumor xenografts using Du-Pan 2 monoclonal antibody. Ann Nucl Med 1988;2:1–6.

73. Klapdor R, Bahlo M, Montz R, Dietal M, Arps H, Bosslet K. Experimental and clinical studies with the new monoclonal antibody 494/32 in pancreatic carcinomas. Digestion 1986;35:31.

74. Kairemo KJA. Radioimmunotherapy of solid cancers. Acta Oncologica 1996;35:343–55.

75. Sharkey RM, Blumenthal RD, Hansen HJ, Goldenberg DM. Biological considerations for radioimmunotherapy. Cancer Res 1990;50:964s–9s.

76. Milenic DE, Yokota T, Filipula DR, et al. Construction, binding properties, metabolism, and tumor targeting of a single-chain Fv derived from the pancarcinoma monoclonal antibody CC49. Cancer Res 1991; 51:6363–71.

77. Zhu H, Baxter LT, Jain RK. Potential and limitation of radioimmunodetection and radioimmunotherapy with monoclonal antibodies. J Nucl Med 1997;38:731–41.

78. Behr TM, Goldenberg DM, Becker W. Reducing the renal uptake of radiolabeled antibody fragments and peptides for diagnosis and therapy: present status, future prospects and limitations. Eur J Nucl Med 1998; 25:201–12.

79. Rolleman EJ, Valkema R, De Jong M, Kooij PP, Krenning EP. Safe and effective inhibition of renal uptake of radiolabeled octreotide by a combination of lysine and arginine. Eur J Nucl Med Mol Imaging 2003;30:9–15.

80. Boerman OC, Kranenborg MHGC, Oosterwijk E, et al. Pretargeting of renal cell carcinoma: improved tumor targeting with a bivalent chelate. Cancer Res 1999;59:4400–5.

81. Le Doussal J-M, Gruaz-Guyon A, Martin M, Gautherot E, Delaage M, Barbet J. Targeting of indium 111-labeled bivalent hapten to human melanoma mediated by bispecific monoclonal antibody conjugates: imaging of tumors hosted in nude mice. Cancer Res 1990;50:3445–52.

82. Nakata B, Nishimura S, Ishikawa T, et al. Prognostic predictive value of ^{18}F-fluorodeoxyglucose positron emission tomography for patients with pancreatic cancer. Int J Oncol 2001;19:53–8.

83. Schuhmacher J, Klivenyi G, Kaul S, et al. Pretargeting of human mammary carcinoma xenografts with bispecific anti-MUC1/anti-Ga chelate antibodies and immunoscintigraphy with PET. Nucl Med Biol 2001;28:821–8.

84. Schuhmacher J, Kaul S, Klivenyi G, et al. Immunoscintigraphy with positron emission tomography: Gallium-68 chelate imaging of breast cancer pretargeted with bispecific anti-MUC1/anti-Ga chelate antibodies. Cancer Res 2001;61:3712–7.